# Spatiotemporal Behavior of Void Collapse in Shocked Solids

Takahiro Hatano

*Center for Promotion of Computational Science and Engineering, Japan Atomic Energy Research Institute, Ibaraki 319-1195, Japan*

(Received 25 June 2003; published 9 January 2004)

Molecular dynamics simulations on a three-dimensional defective Lennard-Jones solid containing a void are performed in order to investigate detailed properties of hot spot generation. In addition to the temperature, I monitor the number of energetically colliding particles which characterizes the intensity of shock-enhanced chemistry. This quantity normalized by void volume is found to saturate for nanoscale voids and to be maximized after voids have completely collapsed. It makes an apparent comparison to the temperature which requires much larger void for the enhancement and becomes maximum during the early stage of the collapse. It is also found that the average velocity and the temperature of ejected molecules inside a cubic void are enhanced during the collapse because of the focusing of momentum and energy towards the centerline of a void.

DOI: 10.1103/PhysRevLett.92.015503 PACS numbers: 62.50.+p, 47.40.Nm, 82.40.Fp

In liquid or solid explosives, it is known that heterogeneities such as bubbles or voids decrease a threshold shock strength above which a detonation takes place. When a shock passes through such defects, they form locally excited regions which are referred to as "hot spots" [1]. Since chemical reactions which turn shocks to detonations are believed to initiate inside such hot spots, the mechanism for the generation of hot spots is important for the understanding of detonations [2]. Since shock waves and void collapse are extremely fast microscopic phenomena, molecular dynamics simulation may be a powerful tool for the study of detailed properties of hot spot initiation. As well as the studies which treat perfect crystals using empirical reactive potentials [3], there are a few works on the interaction between shocks and defects which can yield hot spots [4–7]. For example, Phillips speculated that chemistry would occur in a void below a detonation threshold [6]. However, it is yet to be understood what is essential to the initiation of hot spots. Holian *et al.* recently studied a two-dimensional Lennard-Jones solid with a planar gap which might be regarded as a gap of infinite transverse width [8]. They insisted that the essential ingredients to hot spot generation are the following: (i) enough shock strength for the ejection (spallation) of solid molecules into a void; (ii) compression of ejected particles by the far side of a void. They estimated the overshooting temperature via a straightforward model constructed on the basis of the above conjectures. However, since their estimation is not quantitatively satisfactory (about 3/2 of those obtained by the simulations), the validity of their proposal is not apparent. Moreover, since void collapse is so fast that particles ejected into a void may be far from local equilibrium, it is no longer obvious that the "temperature" could be a fair index for chemistry. We have to monitor other quantities to represent the degree of enhanced chemistry in this situation.

In this Letter, I focus on a dynamical aspect of hot spot generation to understand what is essential to shock-induced chemistry inside a void. Especially, various spatial profiles of the ejected particles are monitored in order to see how the void collapse results in energetic intermolecular collisions which are responsible for chemistry. As for the model, I adopt a three-dimensional fcc crystal whose intermolecular potential is the Lennard-Jones (LJ) one;

$$U(r) = 4\epsilon\left[\left(\frac{\sigma}{r}\right)^{12} - \left(\frac{\sigma}{r}\right)^{6}\right], \tag{1}$$

whose cutoff length is set to be $4.0\sigma$. Throughout this Letter, $\sigma$ and $\epsilon$ are set to unity (the LJ unit). Although one might wonder about the use of nonreactive potential for this kind of issue, this may not be a serious limitation for understanding the dynamical aspect of shock-induced chemistry, i.e., how the coherent (shock) energy relaxes into the thermal energy through the void collapse, which is the main aim of this study. The setup of the system is as follows. The axes of $x$, $y$, and $z$ coincide with $\langle 100\rangle$, $\langle 010\rangle$, and $\langle 001\rangle$ directions, respectively. Although there are various methods used to realize shock waves in molecular dynamics simulations [9], the most popular method is adopted here that a moving piston of infinite mass hits the still target. The velocity of the piston is denoted by $u_p$. Throughout this study, $u_p$ is fixed to be 3 which is strong enough to cause spallation. Shock propagates along the $\langle 001\rangle$ orientation; i.e., $z$ axis. I do not argue orientational dependence which is important to other shock-induced phenomena, such as plastic deformation [10] or phase transitions [11]. The whole system consists of $200 \times 200 \times 200$ unit cells. As usual, periodic boundary conditions are applied to $x$ and $y$ directions. A void consists of blank unit cells, the shape of which is cubic or rectangular solid. Each face is parallel to {100}, {010}, and {001}, respectively. Its typical size ranges from 5 to 40 unit cells

  

for each direction. I fix the initial temperature to be 0.05 and the corresponding density is about 1.053.

Before proceeding to the results, I note the two kinds of averaging methods adopted in this study. One is the average regarding the particles whose initial distance from the upstream wall of the void is less than 5 (about 3 unit cells). Note that all of these particles are eventually ejected into the void after the passage of shock front. I have cross-checked the simulations with different distances from 2 to 15, and the qualitative property obtained below is not influenced by a specific choice of distance. By this method, we can trace the most energetic part of the ejected particles. Most of the results except for Fig. 4 shown below are based on this averaging method. The other method is to take spatial profiles inside a void. This method enables us to see where and when the hot spot generation takes place.

Now let us turn to the results of my simulations. First, time evolutions of the temperature during void collapse are monitored. However, note that the system we are considering is nonequilibrium, where the definitions of thermodynamic quantities including the temperature are precarious [12]. Here I adopt the variance of $z$ velocity as the "temperature," which is denoted by $T_z$. For comparison, I also monitor the variance of $x$ velocity which is denoted by $T_x$. Note that the variances can be different values for different directions; e.g., $T_x$ is smaller than $T_z$ in this situation. Temporal behaviors of $T_z$, $T_x$, and the average $z$ velocity denoted by $v_z$ are shown in Fig. 1. Spallation occurs at $t = 5$ where $v_z$ suddenly increases up to about $2u_p = 6$ (the spall velocity). After the spallation, all of the quantities increase gradually until the ejected molecules collide with the far side of the void (approximately $t = 10$). It should be stressed that $v_z$ increases up to about $2.6u_p$, which means that there is some kind of momentum transfer into the ejecta gas. (We see this acceleration by observing the velocity distribution functions in the next paragraph.) Also it should be noted that the maxima of $T_z$ and $v_z$ are realized simultaneously, which is just before the collision of ejecta gas and the downstream wall of the void. It is not only the compression by the void wall that is responsible for the heating of the ejecta gas but also some kind of focusing of momentum and energy. However, recall that the above results are concerned only with the sample molecules which constitute the proceeding part of ejecta gas. As for the whole gas, observation of the spatial distributions inside the void is needed, which we will see later in detail.

To see the above circumstances regarding the acceleration in detail, velocity distribution function is shown in Fig. 2. Strong displacements from the Maxwellian are seen after the passage of the shock front. Note that a distribution function of $v_x$ is also observed to show an exponential distribution just after the spallation, which then eventually relaxes to the Maxwellian. On the other hand, we can see that the distribution function of $v_z$ has a widely stretched tail for the positive direction, which develops until the collision with the far side of the void. Note that the tail by far exceeds the spall velocity. It is obviously responsible for the increase of $v_z$, since the tail develops only towards the positive direction. The developing tail means that there is a momentum transfer into the ejecta gas, which may be attributed to the focusing. As is visualized in Fig. 3, since the shock pressure also pushes the side wall of the void to form a parabolic surface, the momenta of the collapsing wall can focus onto the centerline of a void, which eventually causes jetting and accelerates the spalled particles. Note that the acceleration during the flight does not happen in a rectangular-solid void with sufficiently large longitudinal length where the parabolic surface is not formed. It is obvious that larger $v_z$ yields more energetic collision, which eventually leads to higher overshooting temperature inside a hot spot. Phillips *et al.* [5] also observed deviations from equilibrium distributions in a collapsing void using a two-dimensional LJ crystal. However, their observation focused only on a relaxation to equilibrium,

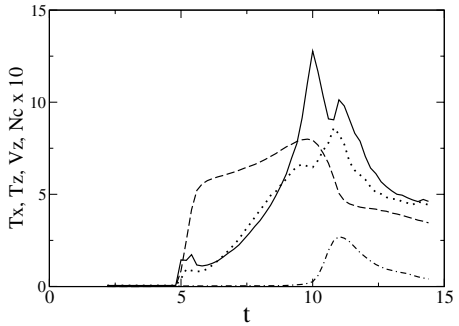


FIG. 1. Temporal behaviors of the longitudinal (solid line) and the transverse (dotted line) temperatures, and the average $z$ velocity (dashed line). The number of energetically colliding particles which is introduced afterwards is also shown by the dot-dashed line (scaled by 10). The sample molecules are those initially located near the upstream wall of the void. (See text.) The void initially consists of $30 \times 30 \times 30$ blank unit cells.

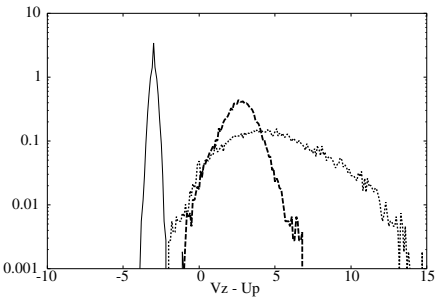


FIG. 2. Velocity distributions of $v_z$. Time ordering is the following: (i) solid lines ($t = 0$; before the spallation), (ii) dashed lines ($t = 6.0$; just after the spallation), and (iii) dotted lines ($t = 9.5$; just before the collision with the far side of the void). Note that $v_z$ is shifted by $-u_p$. All of the parameters including the sample molecules are the same as in Fig. 1.

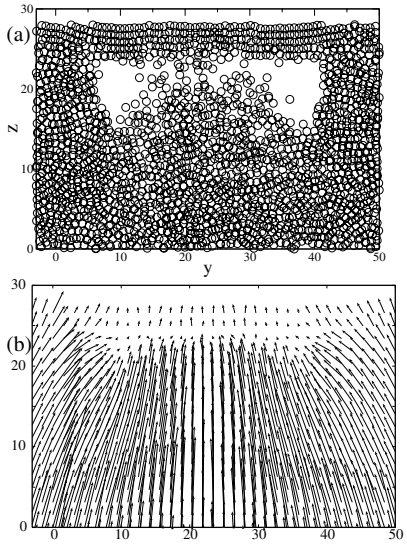


FIG. 3. (a) A slice-cut view (parallel to the {100} plane) of the collapsing void and (b) its velocity vector field. ($t = 9.8$.) A shock propagates upwards.

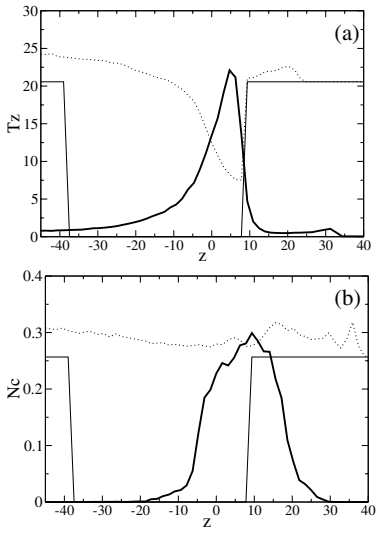


FIG. 4. Spatial profiles of (a) $T_z$ and (b) $N_c$ represented by thick lines together with the density profiles (dotted lines) which are rescaled suitably. [Multiplied by (a) 20 and (b) 0.25.] Each graph is a snapshot at the moment of the maximization of each quantity: (a) $t = 10.0$ for $T_z$ and (b) $t = 11.0$ for $N_c$. The initial density profiles are also imposed (thin lines).

whereas the transition from equilibrium to nonequilibrium is traced here. Also, the positive tail which prevails spall velocity are not seen there, which is the original contribution of this work.

Apart from the temperature and the spall velocity, we then turn to the enhancement of chemical reactions which is our original concern regarding hot spots. Since ejected particles are strongly nonequilibrium as we have seen above, it is no longer expected that the temperature $T_z$ can be a fair index of chemistry. Although chemistry involves many intramolecular degrees of freedom, strong intermolecular collisions are essential to the excitation of those degrees of freedom. Therefore, it is quite natural and direct to count intermolecular collisions for the estimation of chemistry. In this study, I count the couple of particles whose distance is smaller than a certain length, $r_c$. Then the number of the colliding particles is normalized by an initial volume of a void. Hereafter, this intensive quantity is denoted by $N_c$. The values of $r_c$ can be various according to the molecules we are to consider; in this case, I choose $r_c = 0.88$ which corresponds to $U(r_c) = 2.5$. Note that $U(r_c)$ gives an energy threshold for a reaction to occur. However, since LJ potential is adopted here, we do not have the quantitative validity for the choice of $r_c$. Therefore, I cross-check the behaviors of $N_c$ for several values of $r_c$ (0.82, 0.85, 0.88, and 0.91), and no qualitative difference is seen regarding the results obtained in this Letter. Therefore, after these considerations, it may be said that $N_c$ can be a good parameter for chemistry, not to say that it can completely determine go or no go. Typical temporal behavior of $N_c$ is shown in Fig. 1. Note that $N_c$ is zero until the void collapse, which means that strong intermolecular collisions take place only in the void. Also it should be noted that the peaks of $N_c$ and of $T_z$ are not simultaneous: It takes a certain amount of time for $N_c$ to become maximum after the peak of $T_z$. Indeed, this delay means that enhanced chemistry needs higher density than overheating; namely, the delay is a relaxation time for the density to increase in the collapsing void. To confirm this idea, it is observed that the delay becomes longer for larger voids. This situation becomes clear by monitoring spatiotemporal behavior of the density profile inside the void. Figure 4 shows the spatial profiles of $N_c$, $T_z$, and the density, through which we can see in detail where and how the energetic molecular collisions and the overheating take place. Note that these two snapshots are taken at the moments when $T_z$ and $N_c$ become maxima, respectively. The maximum $N_c$ is realized after the whole region of the void has collapsed, while the preceding maximum temperature takes place in the relatively dilute region on the far side of the collapsing void. It is important to notice that $N_c$ becomes maximum after the void has totally collapsed, whereas $T_z$ is maximized at the beginning of collapse. The total collapse yields high density to enhance energetic intermolecular collisions. Therefore the time lag between the maxima of $T_z$ and $N_c$ is the time needed for the total collapse of the void.

The discussions so far finish spatiotemporal behaviors of the ejecta gas and enhanced chemistry. As the final part of my results, I show how the size and the shape of voids affect chemistry. Although voids in real materials can take various forms, it may be decomposed into two essential ingredients: the longitudinal length and the normal cross section. In order to specify which component is important to the initiation of chemical reactions, I check rectangular-solid voids changing the transverse

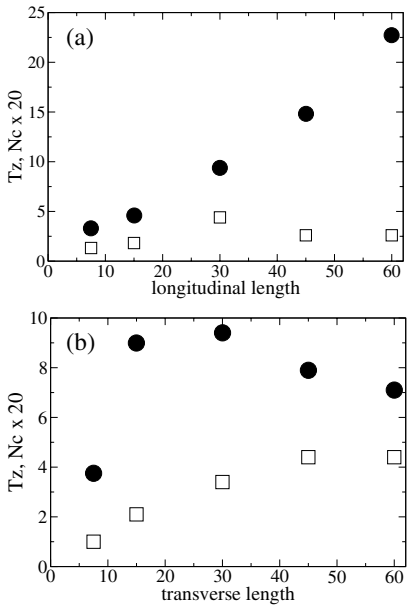


FIG. 5. (a) The longitudinal and (b) the transverse length dependences of $T_z$ (filled circles) and $N_c$ (blank squares, multiplied by 20). The length in the fixed direction of the void is 30 in each case.

and the longitudinal lengths independently. First, I show the longitudinal length dependence with the transverse length (and hence the cross section) fixed. From Fig. 5(a), we can see that $N_c$ is maximized when a void is cubic and decreases for the larger longitudinal length, whereas $T_z$ increases monotonically. As for $T_z$, this result is consistent with [8] where a considerable longitudinal length was needed for the enhancement of temperature. However, the decrease of $N_c$ seems somewhat strange. The possible reasons are the following: (i) Particles to be ejected into a void do not increase much when the longitudinal length is changed; it rather depends on the cross sectional area. (ii) Focusing becomes inefficient when a void is not cubic. On the other hand, the transverse length (i.e., the cross sectional) dependence of $T_z$ and $N_c$ seems quite different from the longitudinal length dependence. In Fig. 5(b), $T_z$ is maximized when the void is cubic, whereas $N_c$ increases to saturate for larger cross sections. It should be stressed that the cross section of $45 \times 45$ (approximately $30 \times 30$ unit cells) is enough for the saturation. The maximization of $T_z$ with a cubic void may be a result of the focusing discussed in the context of acceleration. Also, it should be noticed that a larger cubic void yields higher temperature and $v_z$. The increase of $N_c$ is mainly due to an increase of the number of particles to be ejected into a void. This is also testified to by the fact that higher density (i.e., a complete collapse of void) is required for the increase of $N_c$. A saturated value may depend on the longitudinal length and focusing plays a secondary role for $N_c$ in this case. Hence, it is concluded that the sufficient cross sectional area is important for the enhancement of $N_c$, whereas the longitudinal length is essential for the enhancement of $T_z$. The discrepancy between the behaviors of $N_c$ and $T_z$ again shows that the temperature alone cannot be a reliable index for enhanced chemistry in this nonequilibrium situation. In any case, nanoscale voids (approximately 30 unit cells in each dimension) are enough for the enhancement of energetic intermolecular collisions.

To summarize, through the observations of spatiotemporal behaviors of temperature and density inside a void, we have seen that energetic intermolecular collisions are most likely to occur when a void is totally collapsed. This is not simultaneous with the maximization of temperature which is realized at the beginning of the collapse. This time lag is due to the difference between the optimum densities where each quantity is maximized. The shape of the void affects the two important quantities in different ways; the larger cross sectional area enhances the number of intermolecular collisions normalized by void volume, while larger transverse length enhances temperature. Especially, the number of intermolecular collisions normalized by void volume is found to saturate for nanoscale voids, whereas the enhancement of temperature needs much larger ones. Also, velocity distribution functions are found to deviate from the Maxwellian. These strong nonequilibrium effects must be taken into account for the analysis of spallation phenomena.

The author is grateful to H. Kaburaki and F. Shimizu for helpful discussions and encouragement.

[1] J. P. Dear, J. E. Field, and A. J. Walton, Nature (London) **332**, 505 (1988).
[2] R. Cherét, *Detonation of Condensed Explosives* (Springer-Verlag, New York, 1993).
[3] D.W. Brenner, D. H. Robertson, M. L. Alert, and C. T. White, Phys. Rev. Lett. **70**, 2174 (1993); M. L. Elert, D. M. Deaven, D.W. Brenner, and C. T. White, Phys. Rev. B **39**, 1453 (1989); S.V. Zybin, M. L. Alert, and C. T. White, Phys. Rev. B **66**, 220102 (2002).
[4] P. Maffre and M. Peyrard, Phys. Rev. B **45**, 9551 (1992).
[5] L. Phillips, R. S. Sinkovits, E. S. Oran, and J. P. Boris, J. Phys. Condens. Matter **5**, 6357 (1993).
[6] L. Phillips, J. Phys. Condens. Matter **7**, 7813 (1995).
[7] J.W. Mintmire, D. H. Robertson, and C. T. White, Phys. Rev. B **49**, 14 859 (1994).
[8] B. L. Holian, T. C. Germann, J-B. Maillet, and C. T. White, Phys. Rev. Lett. **89**, 285501 (2002).
[9] B. L. Holian and P. S. Lomdahl, Science **280**, 2085 (1998).
[10] T. C. Germann, B. L. Holian, and P. S. Lomdahl, Phys. Rev. Lett. **84**, 5351 (2000).
[11] V.V. Zhakhovskiĭ, S.V. Zybin, K. Nishihara, and S. I. Anisimov, Prog. Theor. Phys. Suppl. **138**, 223 (2000).
[12] D. Jou, J. Casas-Vázquez, and G. Lebon, *Extended Irreversible Thermodynamics* (Springer, Berlin, 2001), 3rd ed. See Sec. 3.2 for the problems concerning the definition of nonequilibrium temperature beyond local equilibrium.